Open Access Full Text Article

ORIGINAL RESEARCH

Sustained Delivery of Methylsulfonylmethane from Biodegradable Scaffolds Enhances Efficient Bone Regeneration

Yueming Guo[1], Pengpeng Li[2,3], Zongliang Wang [iD][4], Peibiao Zhang[4], Xiaodong Wu[2]

[1]Department of Orthopaedics, Foshan Hospital of Traditional Chinese Medicine, Foshan, 528000, People's Republic of China; [2]Xuzhou Central Hospital, Xuzhou, 221009, People's Republic of China; [3]Graduate School of Bengbu Medical College, Bengbu, 233030, People's Republic of China; [4]Key Laboratory of Polymer Ecomaterials, Changchun Institute of Applied Chemistry, Chinese Academy of Sciences, Changchun, 130022, People's Republic of China

Correspondence: Xiaodong Wu; Peibiao Zhang, Email xiaodongwu2009@163.com; zhangpb@ciac.ac.cn

Introduction: As a popular dietary supplement containing sulfur compound, methylsulfonylmethane (MSM) has been widely used as an alternative oral medicine to relieve joint pain, reduce inflammation and promote collagen protein synthesis. However, it is rarely used in developing bioactive scaffolds in bone tissue engineering.

Methods: Three-dimensional (3D) hydroxyapatite/poly (lactide-*co*-glycolide) (HA/PLGA) porous scaffolds with different doping levels of MSM were prepared using the phase separation method. MSM loading efficiency, in vitro drug release as well as the biological activity of MSM-loaded scaffolds were investigated by incubating mouse pre-osteoblasts (MC3T3-E1) in the uniform and interconnected porous scaffolds.

Results: Sustained release of MSM from the scaffolds was observed, and the total MSM release from 1% and 10% MSM/HA/PLGA scaffolds within 16 days was up to 64.9% and 68.2%, respectively. Cell viability, proliferation, and alkaline phosphatase (ALP) activity were significantly promoted by incorporating 0.1% of MSM in the scaffolds. In vivo bone formation ability was significantly enhanced for 1% MSM/HA/PLGA scaffolds indicated by the repair of rabbit radius defects which might be affected by a stimulated release of MSM by enzyme systems in vivo.

Discussion: Finding from this study revealed that the incorporation of MSM would be effective in improving the osteogenesis activity of the HA/PLGA porous scaffolds.

Keywords: biopolymer, scaffold, drug delivery, sustained release, osteogenesis

Introduction

Bone tissue engineering aims to develop highly porous scaffolds with proper bioactivity to facilitate new bone formation.[1,2] Growth factors have shown favorable function to regenerate bone tissue through regulating cell proliferation, differentiation as well as the formation of mineralized tissue. However, one major disadvantage is that most of them are expensive and can induce cancers.[3,4] A second disadvantage of the growth factors is that the short half-life and unstable characteristic makes them difficult to be delivered within polymer scaffolds.[5] On the contrary, small molecule drugs with distinctive bioactivity are valuable for bio-functionalized polymeric tissue engineering scaffolds owing to their stability and easy processability with polymers.[6–8]

Methylsulfonylmethane (MSM, $(CH_3)_2SO_2$) is an organosulfur compound that can maintain the connective tissues in the human body benefitting from its sulfur content.[9–11] It was reported that co-incubation of MSM and human chondrocytes in moderate severity osteoarthritis could inactive the coding of genes for manufacturing pro-inflammatory cytokines.[12] It demonstrated that MSM was able to protect articular cartilage in patients with osteoarthritis. Joung et al reported that MSM could enhance growth hormone (GH) signaling and osteogenic differentiation of bone marrow mesenchymal stem cells (MSCs).[13] They found that MSM could enhance GH signaling via the pathway of Janus kinase/signal transducers and activators of transcription (Jak2/STAT5b) in osteoblasts and promote osteoblast differentiation through the activation of

4829

Graphical abstract
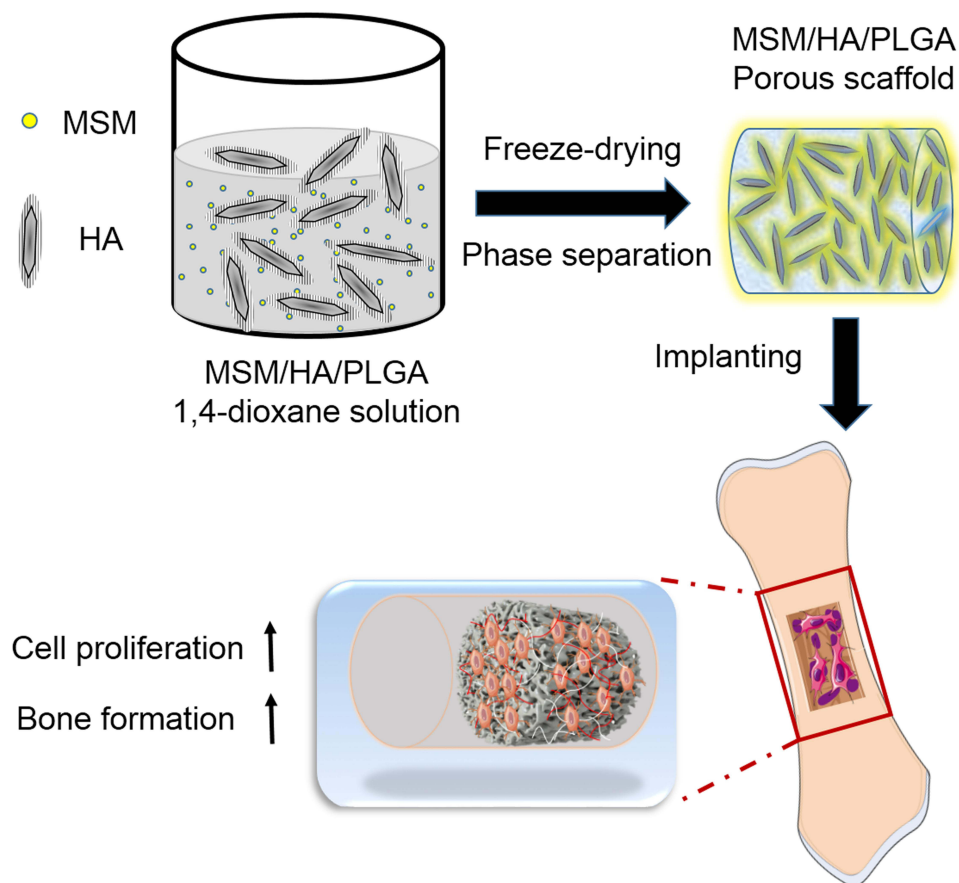
STAT5b in MSCs, thus regulating gene expression of insulin-like growth factor 1 (IGF-1). In another study, the osteogenic differentiation of human periodontal ligament stem cells (hPDLSCs) was evaluated by Ha et al using MSM.[14] The authors observed that MSM could not only promote cell proliferation but also enhance the osteogenic differentiation of hPDLSCs and induce the differentiation of hPDLSCs into osteoblasts as well as bone formation during in vivo bone regeneration. In addition, MSM also increased matrix mineralization and osteogenesis through transglutaminase 2 (TG-2) in stem cells from human exfoliated deciduous teeth (SHED) cells.[15] In addition to the direct application of MSM together with organic silicon and glucosamine sulfate as therapeutic components for mandibular bone defects exhibited positive effect accompanied by bone resorption, MSM has been rarely applied through scaffold-assisted delivery for bone tissue regeneration.[16] In one study, MSM was utilized for the surface coating of porous hydroxyapatite (HA) scaffold.[17] MSM could be released for up to 7 days from the scaffolds. The 2.5% of MSM-coated scaffolds exhibited osteoinductive and osteoconductive potential for bone repair. In our previous work, we prepared MSM-loaded poly (lactide-*co*-glycolide) (PLGA) fibrous mats with a different amount of MSM.[18] The proliferation and extracellular matrix (ECM) formation of chondrocytes were enhanced, and it would be beneficial to cartilage regeneration.

Scaffolds are essential in manipulating cellular differentiation and regenerating new tissues.[5,19] Hydroxyapatite, either containing elements of strontium (Sr) and silicate (SiO_4^{4-}) or not, has been incorporated into biodegradable polymer materials for fabricating composite scaffolds to enhance the bone remodeling process.[20–23] In addition to that, some new biomaterials, especially nano antioxidants, were also developed to be incorporated into scaffolds for tissue regeneration. For example, Marino et al fabricated gelatin/nanoceria nanocomposite electrospun fibers, and the self-regenerative nanoceria-incorporated materials

behaved as a strong antioxidant for inhibiting cell senescence and promoting the neurite sprouting in neuronal regeneration.[24] Nanoceria has also been decorated in polycaprolactone and gelatin (PCLG) blend nanofiber, and it was interesting to note that the nanostructured scaffold could suppress agonist-induced cardiac hypertrophy, suggesting their potential as an antioxidant and anti-hypertrophic cardiac patch.[25] Asghar et al further developed nanoporous zinc-doped hydroxyapatite (Zn-HA) scaffold and the radical scavenging behavior of the nanocomposite scaffold implied great potential as a good antioxidant for application in bone repair.[26] Besides, porous scaffolds with desired properties, such as proper mechanical property, good inner pore architecture, and appropriate bioactivity, are highly demanded for tissue regeneration.[27,28] Therefore, numerous scaffolds were developed with synthetic or natural polymers using a lot of techniques including phase separation,[29] solvent casting-particulate leaching,[30] fiber meshes,[31] gas foaming,[32,33] rapid prototyping,[34] and a series of three-dimensional (3D) or four-dimensional (4D) printing approaches.[35,36] Among these technologies, one of the attractive advantages of phase separation is that a highly interconnected porous structure can be controllably and scalably formed by simply regulating the fabrication parameters, such as polymer concentration, temperature, etc, and bioactive compounds can be directly incorporated without affecting intrinsic biological function.[37] In our previous study, porous nanocomposite scaffolds with honeycomb monolith structure have been fabricated using one-phase solution freeze-drying method.[38]

This work aims to develop an efficient drug delivery and sustained release system for bone regeneration through 3D HA/PLGA porous scaffolds preserving the bioactivity during the low-temperature-assisted fabricating process. As one of the bioactive molecules, MSM was incorporated into the scaffolds with different doping levels. The interaction between mouse pre-osteoblasts (MC3T3-E1) and the MSM-loaded scaffolds, as well as osteogenesis abilities and in vivo bone formation, were systematically investigated.

Materials and Methods
Preparation of MSM-Loaded Porous Scaffolds

A modified frozen and vacuum drying method was used to fabricate the porous scaffolds as reported in our previous study.[38] D, L-Lactide (LA) and glycolide (GA) monomer were obtained from Purac (Netherlands). Poly (lactide-*co*-glycolide) (PLGA, LA:GA= 80:20, Mw = 80,000 g·mol^{-1}) was synthesized as previously reported.[39] Briefly, with the assistance of magnetic stirring and ultrasonic processing, HA (Emperor Nano Material Co., Ltd, Nanjing, China) was uniformly suspended in dehydrated 1,4-dioxane (Sigma-Aldrich, USA), and added to a solution of PLGA/1,4-dioxane (10%, w/v). MSM (Jilin Herun Chemical Co., Ltd, China) was dissolved in acetone (Sigma-Aldrich, USA) and then added into HA/PLGA/1,4-dioxane solution to obtain the MSM/HA/PLGA solution. The volume ratio of acetone and 1.4-dioxane in all the groups was consistent, and the doping levels of MSM in the obtained composites were 0.01%, 0.1%, 1%, and 10%, respectively. The content of HA in all the composites was 10%. The solutions were gently stirred to obtain a homogenous suspension. Then, the obtained composite solutions were frozen within the polypropylene (PP) tubes at 4°C for 24 hours without any protection and then vacuum dried at −4°C to thoroughly remove 1.4-dioxane. HA/PLGA scaffolds without adding MSM were prepared using the same method as control. The samples were kept in a vacuum drying oven.

Observation of Environmental Scanning Electron Microscopy (ESEM)

Brittle-fractured surfaces were obtained by quickly breaking off the frozen samples using liquidized nitrogen (N_2). The gold layer was uniformly sprayed on the surface of the fracture. ESEM (XL30 FEG, Philips) was detected for observing the micro-structure of the different porous scaffolds.

Porosity Analysis

A modified method by displacing liquid was utilized to characterize the porosity of the prepared scaffolds, and three samples for each group were tested.[40] In brief, a scaffold sample with an initial weight of W_i was put in 4 mL of ethanol followed by vacuum treatment until no more bubbles appeared. The volume of ethanol immersed with the scaffold was regarded as V_1. The scaffold containing ethanol was quickly taken away and its weight was recorded as W_f. V_2 was set as the residual volume of ethanol and correspondingly, (V_1-V_2) would be the scaffold volume. The scaffold porosity could

be obtained by calculating the resided volume of ethanol in the scaffold $(W_f-W_i)/\rho_{ethanol}$ ($\rho_{ethanol}$=0.789 g·mL^{-1}). Thus, the opening porosity could be determined as follows:

Porosity=$[(W_f-W_i)/\rho_{ethanol}]/(V_1-V_2)$

Compressive and Bending Strength

The compressive strength and three-point bending strength of the scaffolds were evaluated using a universal testing machine (Instron 1121, UK) as previously reported.[41] Cylinder-shaped samples with a diameter of 10 mm and a length of 10 mm were tested for compressive strength with a 2 mm·min^{-1} of crosshead speed. Similar cylinder-shaped samples with a diameter of 10 mm and a length of 30 mm were tested for three-point bending strength with a 5 mm·min^{-1} of crosshead speed. The compressive strength and bending strength were calculated according to standards SS-EN ISO 178:2019 and SS-EN ISO 604:2002, respectively. Three replicates were tested for each condition.

Water Contact Angle Tests

HA/PLGA composite films with different content of MSM were prepared on the cover slides which were pretreated using 2% dimethyldichlorosilane (DMDC).[42] Static water contact angle (Krüss DSA 10, Germany) was detected by measuring the water contact angle on three different locations of the composite films according to ASTM D5946 to obtain the average values as the final results.[43] A water droplet of 6 μL was dropped fulfilling the requirements of the ASTM standards ranging from 5 to 8 μL.

MSM Loading Efficiency and in vitro Release

Twenty mg of MSM-loaded composite scaffolds were accurately weighed and dissolved in 10 mL nitric acid (HNO$_3$, Sigma-Aldrich, USA).[44] The constant volume was adjusted to 25 mL using deionized water as required by the protocol. The quantitation of sulfur (W_S) was detected through the inductively coupled plasma atomic emission spectroscope (ICP-OES, Leeman Prodigy High Dispersion ICP, USA). The following equation could be used to calculate the actual MSM amount (W_{MSM}) in each sample:

$W_{MSM}= W_S \times M_{MSM}/M_{S,}$

M_{MSM}: molar mass of MSM, 94 g·mol^{-1}. M_S: molar mass of sulfur, 32 g·mol^{-1}. Three samples for each group were tested.

For in vitro MSM release, 200 mg of MSM-loaded composite scaffolds were immersed in 10 mL of phosphate-buffered saline (PBS, pH=7.2) at 37°C shaking constantly (100 rpm).[44] The released liquid was taken out at different time and refreshed with fresh PBS. The released sulfur quantitation (W_S) was detected through ICP-OES. Then, the released MSM (W_{MSM}) was calculated according to the above equation. Four samples for each group were tested.

Cell Culture in the Porous Scaffolds

MC3T3-E1 cells (Institute of Biochemistry and Cell Biology, Shanghai Institutes for Biological Sciences, Chinese Academy of Sciences) were cultured using Dulbecco's Modified Eagle Medium (DMEM, Gibco, USA) supplemented with 10% fetal bovine serum (FBS, Gibco, USA), 100 mg·L^{-1} penicillin (Sigma-Aldrich, USA) and 63 mg·L^{-1} streptomycin (Sigma-Aldrich, USA) at 37 °C and 5% CO$_2$ of humidified atmosphere. The medium was refreshed every 2 days. The cells were digested by a solution of 0.25% trypsin-EDTA (Sigma-Aldrich, USA), followed by centrifugation and resuspension in DMEM. The scaffolds with a diameter of 10 mm and a height of 5 mm were put in 24-well plates and sterilized with ultraviolet rays (UV) for 60 min and pretreated in ethanol (70%) for 15 min. Then, the samples were rinsed thrice with PBS and immersed in DMEM for another 10 min. Cells with a density of 10×10^4 cells in a 100 μL medium were seeded on each scaffold and cultured for 4 hours for initial cell attachment. After that, 1 mL fresh DMEM was gently dropped onto each sample and incubated at the same culturing condition.

Cell penetration into the scaffolds was characterized by fluorescence microscopy (TE2000-U, NIKON, Japan). Glutaraldehyde (2.5%) was utilized to fix cells for 15 min, and the nucleus was stained using 4',6-diamidino-2-phenylindole (DAPI, Beijing Solarbio Science & Technology Co., Ltd, China) to investigate the cellular behaviors inside the scaffolds.

Cell Proliferation and Alkaline Phosphatase (ALP) Activity Assay

MC3T3-E1 osteoblast proliferation within the composite scaffolds was determined by using 3-(4,5-dimethyl-2-thiazolyl)-2,5-diphenyl-2-H-tetrazolium bromide (MTT, Sigma-Aldrich, USA) assay.[41] In brief, three replicates of the porous scaffolds were seeded with MC3T3-E1 cells at a density of 4×10^4 cells in a 100 μL medium followed by adding 1 mL of DMEM 4 hours later in 24-well tissue culture plates (Costar). The cells were cultured for 3, 7, and 14 days at 37 °C and 5% CO_2. The medium was refreshed every 2 days. MTT solution (100 μL, 5 mg/mL in PBS) was added to each sample and continued to incubate for another 4 hours. The medium was replaced by acidified isopropanol (750 μL, 2 mL 0.04 N HCl in 100 mL isopropanol) for solubilizing the converted dye. Then, 200 μL of the solution was transferred to a 96-well plate to measure the optical density at 540 nm wavelength using a Full Wavelength Microplate Reader (Infinite M200, TECAN). The average value of three replicates for each sample was obtained.

The p-nitrophenol phosphate assay kit (pNPP, Sigma-Aldrich, USA) was used to determine the alkaline phosphatase (ALP) activities of MC3T3-E1 cells incubated in the different scaffolds for 7 days.[45] MC3T3-E1 cells were rinsed thrice and lysed using lysis buffer followed by freezing and thawing. Then, 200 μL of pNPP solution was added into each well in the dark and incubated at 37 °C for 30 min according to the manufacturer's protocol. The optical density (OD) at 405 nm was measured through a Full Wavelength Microplate Reader (Infinite M200, TECAN). The total content of protein was detected with a bicinchoninic acid (BCA, Sigma-Aldrich, USA) protein assay kit for normalization of ALP activity value. Three samples for each group were tested. The average values were obtained as the ALP activities.

Bone Defect Repair

A rabbit radius with a critical size defect was created for evaluating the bone regeneration ability of the MSM-incorporated scaffolds.[46] Thirty-six New Zealand white rabbits (male, 2 months old, 2.5–3.0 kg) were provided by the Institute of Experimental Animal of Jilin University. The animal experiments were approved by the Jilin University Animal Care and Use Committee. The rabbits were raised in the Institute of Experimental Animals of Jilin University, based on the institutional guidelines for the care and use of laboratory animals. Animals were randomly divided into six groups (n=6 per group) and anesthetized by intramuscularly injecting xylazine hydrochloride ($0.2 \ mL \cdot kg^{-1}$).[47] The porous scaffolds were placed into the rabbit defects with a pure defect without transplanting any scaffolds as the blank control. The wounds were carefully sutured layer-by-layer. After the surgical operation, the rabbits were freely raised in the cages with a daily intramuscular injection of penicillin (400,000 units each) for 7 days. All the wounds gradually healed without any post-surgery complications. All the animals were euthanized by asphyxiating with carbon dioxide after 12 weeks.

The healing process of bone defect was traced by taking digital radiographs (DR) using CR 400 plus Filmless Radiology System (KODAK, USA) at 4 and 12 weeks after surgery. The digital radiographs were further relatively quantified based on the Lane–Sandhu scoring system as shown in Supplementary Table 1.[48] At least six samples were tested for each group. Five independent examiners were trained in the Lane–Sandhu system and all the points were individually given according to the degree of bone formation, connections, and bone marrow recanalization. Four points indicate fully bone formation. Zero points mean failure of bone formation. Based on the integrity of the fracture line, 0, 2, and 4 points are given to reveal the connection degree. Four points indicate no fracture line can be observed. On the contrary, 0 point can be given. The degree of recanalization for bone marrow recanalization can be identified by giving 0, 2, or 4 points.

Statistical Analysis

All the data were analyzed using Origin 8.0 (OriginLab Corporation, USA), and the mean ± standard deviation (SD) was shown. Statistical analysis was performed to evaluate the variance (one-way ANOVA, Origin 8.0). A p-value less than 0.05 was regarded as statistically significant.

Results

Porous Scaffold Characterization

The inner structure of the porous scaffolds of HA/PLGA and MSM/HA/PLGA was detected by ESEM as shown in Figure 1. A similar highly porous microstructure was observed in all the scaffolds. The pores in all the scaffolds were uniformly
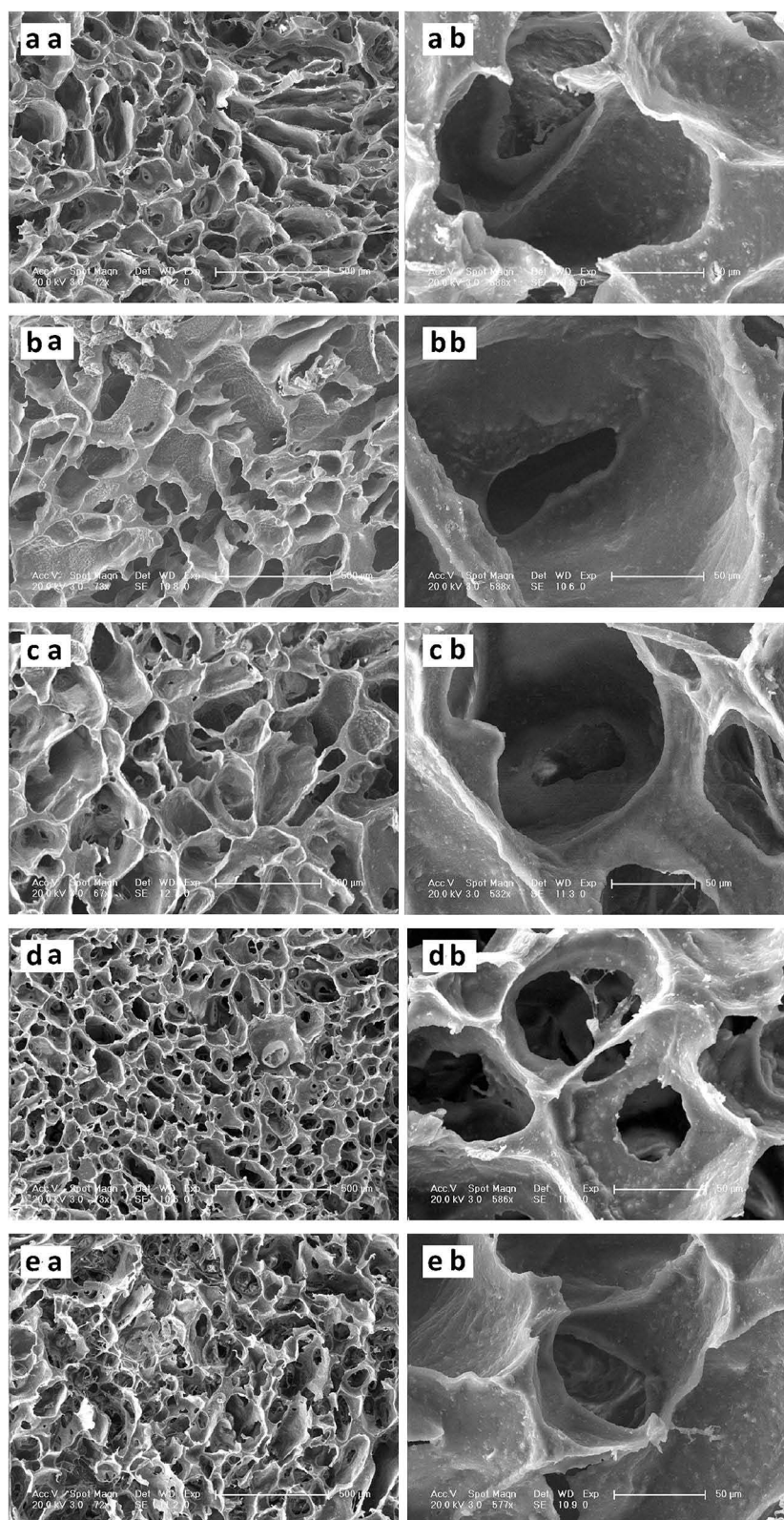
Figure 1 ESEM images of porous scaffolds of HA/PLGA (a), 0.01% MSM/HA/PLGA (b), 0.1% MSM/HA/PLGA (c), 1% MSM/HA/PLGA (d) and 10% MSM/HA/PLGA (e). The images are shown at low (−1) and high (−2) magnifications. Bar lengths are 500 μm and 50 μm, respectively.

distributed with interconnected pore structures (Figure 1 aa to ea). Observation under a high magnification showed that rough surfaces were noted in all the scaffolds due to the existence of nano-HA particles (Figure 1 ab to eb).

The porosity of the different scaffolds is given in Table 1. Although the addition of MSM slightly increased the scaffold porosity, no significant difference was observed ($p > 0.05$). Therefore, it could be concluded that doping MSM did not have an apparent effect on the porosity of composite scaffolds.

As shown in Table 2, the water contact angle of the composite films decreased gradually with increasing the content of MSM. The water contact angle of 1% MSM/HA/PLGA film was lower than the samples of HA/PLGA, 0.01% and 0.1% MSM/HA/PLGA films ($p < 0.05$). The water contact angle of 10% MSM/HA/PLGA film was also significantly lower than that of the samples of HA/PLGA 0.01% and 0.1% MSM/HA/PLGA films ($p < 0.05$). However, there was no significant difference between 1% and 10% MSM/HA/PLGA films ($p > 0.05$).

Mechanical Properties

The compressive and bending strength of HA/PLGA and MSM/HA/PLGA porous scaffolds were shown in Table 3. The compressive strength decreased slightly with the increasing amount of MSM up to 1% without significant differences ($p > 0.05$). The scaffold of 10% MSM/HA/PLGA showed the minimum compressive strength ($p < 0.05$). Similarly, decreased bending strength was observed as the content of MSM increased and the 10% MSM/HA/PLGA composite scaffold showed the lowest bending strength ($p < 0.05$).

Table 1 Porosity of the Different Scaffolds

Scaffolds	Porosity (%)
HA/PLGA	85.1 ± 0.5
0.01% MSM/HA/PLGA	87.5 ± 1.2
0.1% MSM/HA/PLGA	90.6 ± 0.9
1%MSM/HA/PLGA	88.1 ± 1.0
10% MSM/HA/PLGA	87.2 ± 1.1

Table 2 Water Contact Angle of the Different MSM-Incorporated Films

Films	Contact Angle (Deg.)
HA/PLGA	78.2 ± 0.68
0.01% MSM/HA/PLGA	77.8 ± 0.71
0.1% MSM/HA/PLGA	77.1 ± 0.50
1%MSM/HA/PLGA	71.3 ± 0.58[a]
10% MSM/HA/PLGA	68.6 ± 1.12[b]

Notes: [a,b]Indicated $p < 0.05$. a: 1% MSM/HA/PLGA vs HA/PLGA, 0.01% and 0.1% MSM/HA/PLGA; b: 10% MSM/HA/PLGA vs HA/PLGA, 0.01% and 0.1% MSM/HA/PLGA.

Table 3 Compressive and Bending Strength of the Different MSM-Incorporated Scaffolds

Scaffolds	Compressive Strength (MPa)	Bending Strength (MPa)
HA/PLGA	3.23 ± 0.16	1.28 ± 0.08
0.01% MSM/HA/PLGA	3.18 ± 0.14	1.18 ± 0.10
0.1% MSM/HA/PLGA	3.22 ± 0.20	1.20 ± 0.13
1%MSM/HA/PLGA	2.96 ± 0.13	1.02 ± 0.06
10% MSM/HA/PLGA	2.18 ± 0.10*	0.65 ± 0.07*

Note: *$p < 0.05$, compared with the other groups.

MSM Loading Efficiency and in vitro Release

The loading efficiency of MSM in the composite scaffolds is shown in Supplementary Table 2. The actual content of MSM in the composite scaffolds gradually increased with increasing the feed weight fraction. The incorporated MSM content was accordingly less than the theoretical amount owing to the sublimation of MSM during the fabrication process.

Two groups of the MSM-incorporated scaffolds were evaluated for drug release as shown in Figure 2. The released MSM from 1% and 10% MSM/HA/PLGA scaffolds increased to about 60% during the first 48 hours. The total amount of MSM released from 1% and 10% MSM/HA/PLGA scaffolds were 64.9% and 68.2% at 384 hours, respectively. It demonstrated that MSM could be sustainably released from the MSM/HA/PLGA scaffolds. The sustained release of MSM from the porous scaffolds can prolong its therapy effect on the regulation of cellular metabolism for bone regeneration or osteoarthritis in vivo.

Cell Distribution and Proliferation in the Porous Scaffolds

The spatially distributed cells in the scaffolds were evaluated through staining cell nucleus with DAPI after being cultured for 7 days. Cell nuclei were found in the scaffolds, especially for the 0.01%, 0.1%, and 1% MSM/HA/PLGA scaffolds (Supplementary Figure 1B–D). HA/PLGA and 10% MSM/HA/PLGA scaffolds (Supplementary Figure 1A and E) showed similar cell amount and distribution which was much less than the other groups.

Figure 3 shows that the cell proliferation in MSM-incorporated scaffolds was better than in the HA/PLGA scaffolds on days 3, 7, and 14, especially for the 0.1% MSM/HA/PLGA scaffolds. The results indicated that cell proliferation was promoted with the incorporation of MSM during cell culture.

ALP Activity

Cellular ALP activity was evaluated with the different doping levels of MSM in the composite scaffolds (Figure 4). On day 7, ALP activities were elevated in all the MSM-loaded scaffolds with a significant difference ($p < 0.05$). Furthermore, the ALP activity of 0.1% MSM/HA/PLGA scaffolds was the highest among all the MSM-incorporated groups ($p < 0.05$). It suggested the osteoinductivity of MSM-incorporated scaffolds.

In vivo Bone Formation of MSM-Incorporated Scaffolds

Lastly, porous scaffolds loading of MSM was transplanted in critical-sized bone defects for bone regeneration. Bone formation was examined using DR at 4 and 12 weeks after transplantation (Figure 5). Four weeks post-surgery, only a small bone callus was observed at the edge of the bone defect for blank control groups (Figure 5 aa). However, bone callus emerged in the scaffold-transplanted defects (Figure 5 ba, ca, da, ea, and fa). The bone defects for 0.01%, 0.1%, and 1% MSM/HA/PLGA scaffolds were found to be bridged with new bone tissue formation (Figure 5 ca, da, and ea).
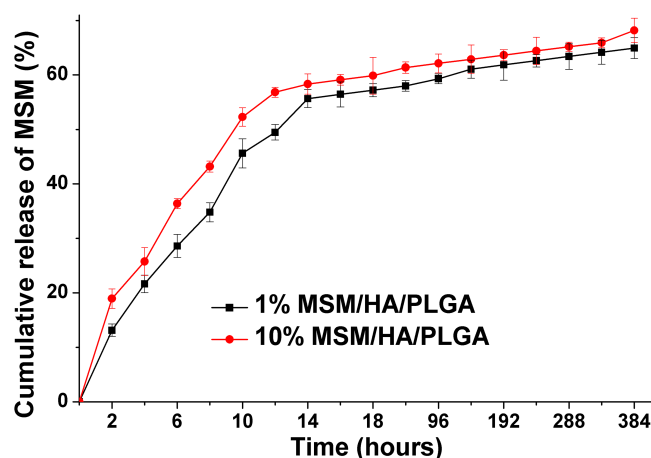

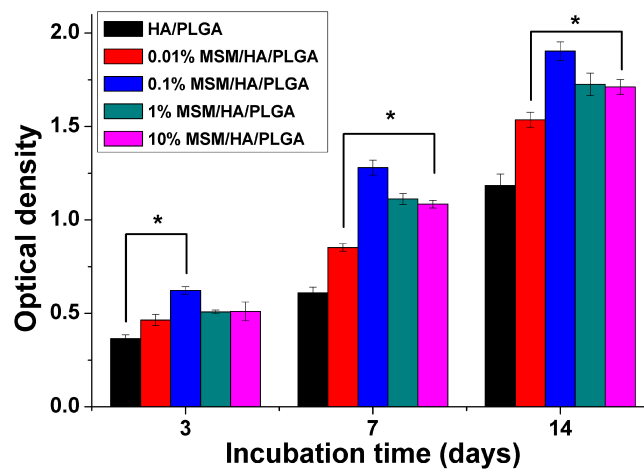**Figure 2** Cumulative release of MSM from 1% and 10% MSM/HA/PLGA scaffolds in PBS for 384 hours.

Figure 3 The proliferation of MC3T3-E1 cells cultured in the different scaffolds for 3, 7, and 14 days. Mean ± SD, n=4. *Significant difference, $p < 0.05$.
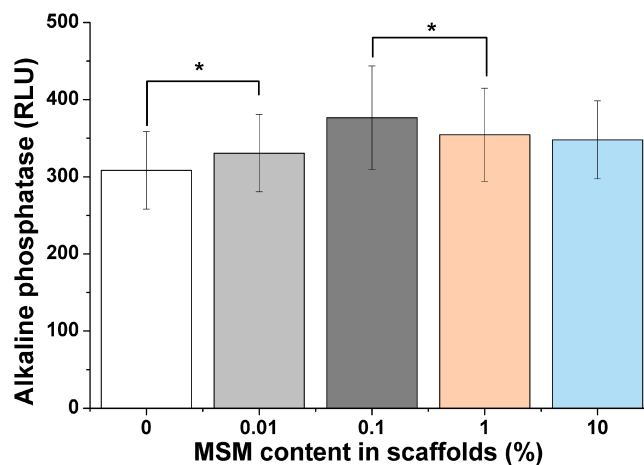

Figure 4 Alkaline phosphatase activity of MC3T3-E1 cells cultured in the different scaffolds for 7 days. Mean ± SD, n=3. *Significant difference, $p < 0.05$.

While an obvious gap between bone formation in the groups of HA/PLGA and 10% MSM/HA/PLGA scaffolds was also observed (Figure 5 ba and fa). The group of 1% MSM/HA/PLGA (Figure 5 ea) showed the highest density of radiograph, and the group of 0.01% MSM/HA/PLGA (Figure 5 ca) exhibited the largest area of newly formed bone.

As confirmed by DR, new bone formation was not remarkable for the blank control and HA/PLGA groups at 12 weeks post-surgery (Figure 5 ab and bb). In contrast, transplantation of the MSM-loaded scaffolds exhibited a great amount of bone formation than HA/PLGA scaffolds or blank control at 12 weeks. Implanting with the MSM-loaded scaffolds showed bridged defects with more new bone formation (Figure 5 cb, db, eb, and fb). Lane–Sandhu scoring results are shown in Figure 6. The score of 0.1% MSM/HA/PLGA group was the highest one among all the groups without a significant difference at 4 weeks post-surgery ($p > 0.05$). The scores obtained from 1% MSM/HA/PLGA scaffolds was higher than that of other groups with significant difference except for the 10% MSM/HA/PLGA group at 12 weeks post-surgery ($p < 0.05$). However, no statistically significant difference was found among the rest groups ($p > 0.05$).

Discussion

Tissue engineering aims to create engineered tissues and organs using biodegradable scaffolds and various functional nanomaterials.[49,50] To this end, developing 3D architecture with ideal pore architecture is critical for cell behaviors and the formation of new tissues presenting efficient delivery of drugs, biological molecules as well as stem cells.[51,52]
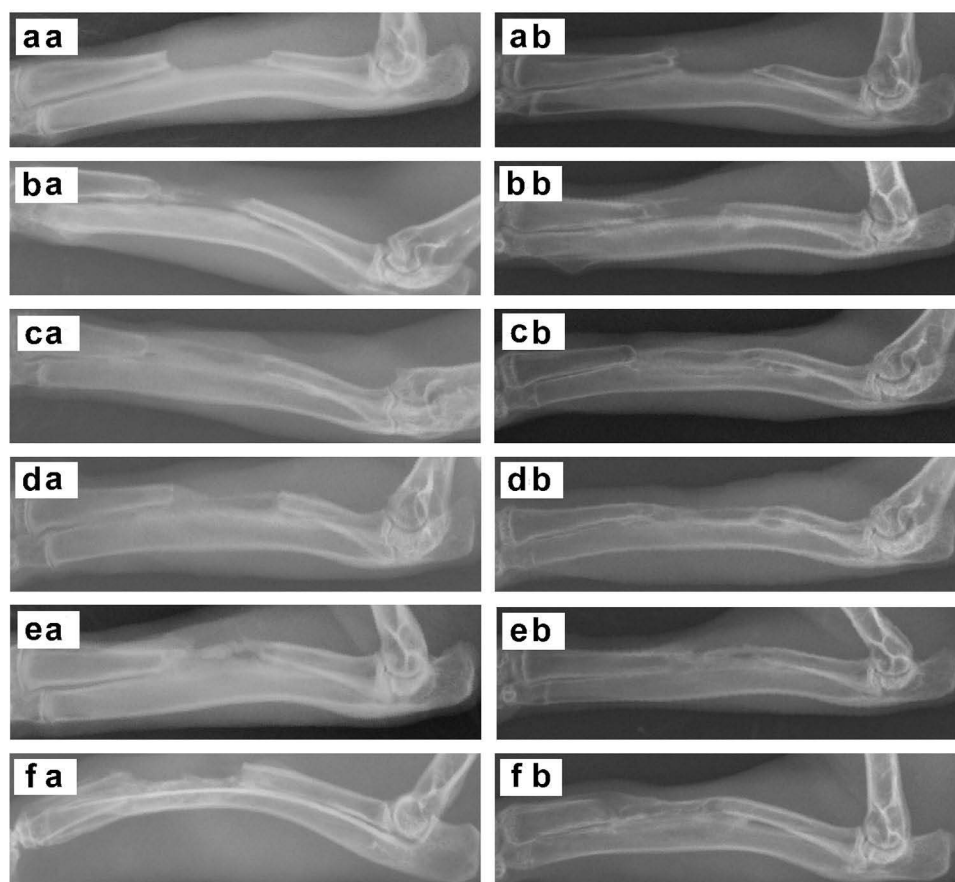
Figure 5 Representative DR images of rabbit radius defects implanted with the different scaffolds 4 weeks (−1) and 12 weeks (−2) post-surgery: blank control (a), HA/PLGA (b), and HA/PLGA containing MSM: 0.01% (c), 0.1% (d), 1% (e) and 10% (f).
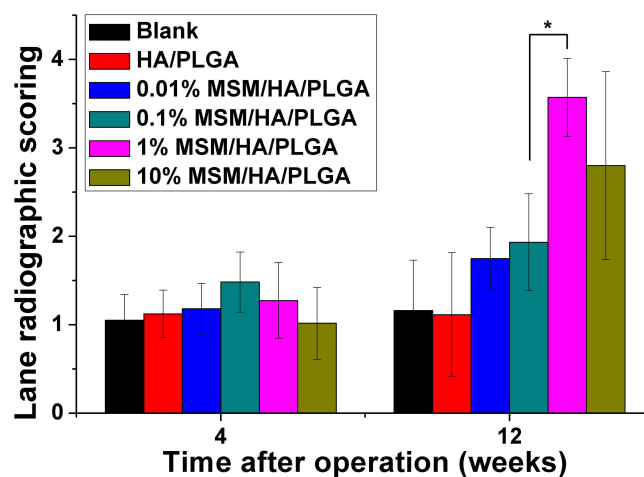

Figure 6 Lane–Sandhu radiographic scores of rabbit radius defects of blank control and implanted with the different scaffolds at 4 and 12 weeks post-surgery. *Significant difference, $p < 0.05$.

Therefore, pore size, porosity, the roughness of pore surfaces, and bioactivity of scaffolds play a critical role in regenerating tissues. In this study, highly porous scaffolds were fabricated using the phase separation method, and frozen solvent was conducive to the formation of the pore structures as described in our previous report.[38] Observation by ESEM showed that all the scaffolds with or without MSM incorporation exhibited similar pore structures with a pore

sizes of 50–250 μm and the pores of the scaffolds were uniformly distributed with interconnected micro-structure, implying that the incorporation of MSM did not influence the porous structure of scaffolds. Additionally, the porosity of the scaffolds was also not influenced by the incorporation of MSM. The lower compressive and bending strength of the scaffolds doped with 10% MSM implied that a higher amount of MSM meant less polymer matrix resulting in worse mechanical properties.[53] The results indicated that higher level incorporation of MSM influenced the mechanical properties of the composite scaffolds, especially for a 10% amount of MSM in the composite scaffolds. This is very consistent with the reported results that the expression of osteogenesis markers of hDPSCs was upregulated by the addition of simvastatin (SIM) and HA into the nanofibrous scaffolds of poly (ε-caprolactone) (PCL)/poly lactic acid (PLLA).[54] It suggested that better cell response could be achieved by combining small molecule drugs (eg, MSM) with HA nanoparticles in polymer matrices.

Previous studies demonstrated that the roughness and wettability of the pore surface were closely related to cell interaction with the scaffolds.[55–57] The pore wall surfaces of all the obtained scaffolds were rough due to the existence of HA nanoparticles. The pore surface roughness and osteoconductivity would be beneficial for cell viability, spreading, proliferation and differentiation.[58,59] The significantly decreased water contact angle of MSM-incorporated scaffolds, especially for the 1% and 10% groups, indicated that the surface wettability was substantially enhanced by the efficient cargo loading of bioactive substances. The cell proliferation was significantly enhanced by adding MSM in the scaffolds, especially for the content of MSM was more than 0.01%. While the cell proliferation of 0.1% MSM/HA/PLGA scaffolds was further better than the groups of 1% and 10% without significant difference. The cell amount evaluated by nucleus staining showed that the cell distribution in the scaffolds was more favorable for the 0.01%, 0.1%, and 1% MSM/HA/PLGA scaffolds, which was consistent with the MTT results and it indicated that the appropriate amount of MSM in the porous scaffold would be beneficial to cell proliferation. This was consistent with previous studies that MSM-incorporated electrospun fibers promoted chondrocytes' proliferation and extracellular formation in vitro,[18] the incubation of 10 mg·mL^{-1} MSM was nontoxic to murine macrophages for 24 hours,[60] and no adverse effects or mortality were observed when orally administering MSM with 1.5 g·kg^{-1}·day^{-1} for 90 days in rats.[61]

Among the important osteogenic markers, ALP activity is critical during the early time points of osteogenesis.[62] The ALP activity of MC3T3-E1 cells subjected to the scaffolds on day 7 was significantly enhanced in the MSM-loading scaffolds in comparison with HA/PLGA scaffolds, indicating that MSM was able to induce an up-regulating of ALP which was relevant to the early performance of osteogenesis differentiation.[63] Among the MSM-doped groups, the highest cellular ALP activity was observed in the 0.1% MSM/HA/PLGA scaffold. It was reported that MSM could enhance growth hormone signaling and osteoblast differentiation in MSCs.[13] The results indicated that an appropriate amount of MSM in the porous scaffold could be helpful for osteodifferentiation. Similar to this study, Ghandforoushan et al supplemented TGF-β1 into a PLGA-collagen scaffold with PLGA-poly (ethylene glycol)-PLGA nanoparticles as delivery vehicles to enhance the chondrogenic differentiation of hDPSCs.[64] In all, it can be expected that the tissue engineering strategy by combining 3D biomimetic structure and sustained release of therapeutic agents would represent technological advancements for tissue repair and clinical therapy.

Therefore, after in vitro evaluation of MSM-loaded composite scaffolds, a rabbit radius defect model was developed to investigate in vivo bone formation ability. The MSM-incorporated scaffold regenerated a large amount of bone than the blank control and HA/PLGA group both at 4 and 12 weeks. Moreover, the DR images and Lane–Sandhu scores demonstrated that the 1% MSM/HA/PLGA scaffold exhibited strong osteointegration than the other groups. Combined with the above in vitro cellular evaluation, it was interesting to be noted that an appropriate doping level of bioactive substance displayed better in vivo bone regeneration ability which was similar to our previous observation. That was a meaningful phenomenon that moderate grafting amount of LAc oligomer on HA nanoparticles within polymer matrix exhibited preferable osteogenesis ability, neither the highest nor the lowest grafting amounts.[65] It could be speculated that the degradation of the PLGA matrix was accelerated to a certain extent by enzyme systems in vivo and the stimulated release of MSM with an appropriate level further promoted bone formation. The detailed mechanism of drug release from the scaffolds assisted by in vivo enzymic microenvironment and their potential enhancement for bone regeneration will be systematically evaluated in our following work. In a word, MSM incorporation promoted the bioactivity of porous HA/PLGA scaffolds, and it was in consistence with previous studies.[13,18]

Thus, we herein demonstrate that MSM incorporation is a meaningful strategy to enhance the bioactivity of porous scaffolds for repairing bone defects. The MSM-loaded bioactive scaffolds in this study would be beneficial for the therapy of osteoarthritis, large area bone defect, or nonunion of bone. In our future work, the mechanism of osteogenesis and more biological functions of MSM-loaded scaffolds need to be further investigated through a lot of biological experiments both in vitro and in vivo.

Conclusions

In this study, MSM-loaded porous scaffolds were successfully prepared using the phase separation method. The incorporation of MSM in the scaffolds improved cell proliferation and cellular ALP activity in vitro. Moreover, animal tests revealed that MSM/HA/PLGA scaffolds showed great osteogenesis properties and promoted bone formation in vivo, especially for the 1% MSM/HA/PLGA scaffolds. Finding from this study suggests that the porous scaffold fabricated through phase separation is an efficient platform for cargo loading of bioactive small molecules to generate functionalized implants. Therefore, the MSM/HA/PLGA porous scaffolds are promising candidates in bone tissue engineering and orthopedic applications.

Acknowledgments

Disclosure

There are no conflicts of interest to declare.

References

1. Langer R. Perspectives and challenges in tissue engineering and regenerative medicine. *Adv Mater*. 2009;21(32–33):3235–3236. doi:10.1002/adma.200902589

2. Liu SQ, Wu XY, Hu JP, Wu ZZ, Zheng YY. Preparation and characterisation of a novel polylactic acid/hydroxyapatite/graphene oxide/aspirin drug-loaded biomimetic composite scaffold. *N J Chem*. 2021;45(24):10788–10797. doi:10.1039/D1NJ01045J

3. Major JM, Pollak MN, Snyder K, Virtamo J, Albanes D. Insulin-like growth factors and risk of kidney cancer in men. *Br J Cancer*. 2010;103 (1):132–135. doi:10.1038/sj.bjc.6605722

4. Solarek W, Czarnecka AM, Escudier B, Bielecka ZF, Lian F, Szczylik C. Insulin and IGFs in renal cancer risk and progression. *Endocr Relat Cancer*. 2015;22(5):R253–R264. doi:10.1530/ERC-15-0135

5. Eugenis I, Wu D, Rando TA. Cells, scaffolds, and bioactive factors: engineering strategies for improving regeneration following volumetric muscle loss. *Biomaterials*. 2021;278:121173. doi:10.1016/j.biomaterials.2021.121173

6. Li GL, Yang B, Gu CT. Drug self-gating fluorescent nanoparticles for pH-responsive doxorubicin delivery. *J Mater Sci*. 2020;55(2):738–747. doi:10.1007/s10853-019-04020-7

7. Sun P, Zhang QQ, Nie W, et al. Biodegradable mesoporous silica nanocarrier bearing angiogenic qk peptide and dexamethasone for accelerating angiogenesis in bone regeneration. *ACS Biomater Sci Eng*. 2019;5(12):6766–6777. doi:10.1021/acsbiomaterials.9b01521

8. Pekozer GG, Akar NA, Cumbul A, Beyzadeoglu T, Kose GT. Investigation of vasculogenesis inducing biphasic scaffolds for bone tissue engineering. *ACS Biomater Sci Eng*. 2021;7(4):1526–1538. doi:10.1021/acsbiomaterials.0c01071

9. Butawan M, Benjamin RL, Bloomer RJ. Methylsulfonylmethane: applications and safety of a novel dietary supplement. *Nutrients*. 2017;9(3):290. doi:10.3390/nu9030290

10. Sousa-Lima I, Park SY, Chung M, et al. Methylsulfonylmethane (MSM), an organosulfur compound, is effective against obesity-induced metabolic disorders in mice. *Metab Clin Exp*. 2016;65(10):1508–1521. doi:10.1016/j.metabol.2016.07.007

11. Amiel D, Healey RM, Oshima Y. Assessment of methylsulfonylmethane (MSM) on the development of osteoarthritis (OA): an animal study. *FASEB J*. 2008;22:1094.1093. doi:10.1096/fasebj.22.1_supplement.1094.3

12. Oshima Y, Da J, Theodosakis J. Theodosakis. The effect of distilled methylsuldonylmethane (MSM) on human chondrocytes in vitro. *Osteoarthr Cartil*. 2007;15(SupplementC):C123. doi:10.1016/S1063-4584(07)61846-9

13. Joung YH, Lim EJ, Darvin P, et al. MSM enhances GH signaling via the Jak2/STAT5b pathway in osteoblast-like cells and osteoblast differentiation through the activation of STAT5b in MSCs. *PLoS One*. 2012;7(10):e47477. doi:10.1371/journal.pone.0047477

14. Ha S-H, Choung P-H. MSM promotes human periodontal ligament stem cells differentiation to osteoblast and bone regeneration. *Biochem Biophys Res Commun*. 2020;528:160–167. doi:10.1016/j.bbrc.2020.05.097

15. Aljohani H, Senbanjo LT, Chellaiah MA. Methylsulfonylmethane increases osteogenesis and regulates the mineralization of the matrix by transglutaminase 2 in SHED cells. *PLoS One*. 2019;14(12):e0225598. doi:10.1371/journal.pone.0225598

16. Rosa FSD, Stuepp RT, Modolo F, Biz MT. Effect of organic silicon, methylsulfonylmethane, and glucosamine sulfate in mandibular bone defects in rats. *Microsc Res Tech*. 2017;80(11):1161–1166. doi:10.1002/jemt.22911

17. Ryu J-H, Kang T-Y, Shin H, Kim K-M, Hong M-H, Kwon J-S. Osteogenic properties of novel methylsulfonylmethane-coated hydroxyapatite scaffold. *Int J Mol Sci*. 2020;21:8501. doi:10.3390/ijms21228501

18. Wang Z, Wang Y, Zhang P, Chen X. Methylsulfonylmethane-loaded electrospun poly (lactide-co-glycolide) mats for cartilage tissue engineering. *RSC Adv*. 2015;5:96725. doi:10.1039/C5RA19183A

19. Qu YC, Lu KY, Zheng YJ, et al. Photothermal scaffolds/surfaces for regulation of cell behaviors. *Bioact Mater*. 2022;8:449–477. doi:10.1016/j.bioactmat.2021.05.052

20. Surmenev RA, Shkarina S, Syromotina DS, et al. Characterization of biomimetic silicate- and strontium-containing hydroxyapatite microparticles embedded in biodegradable electrospun polycaprolactone scaffolds for bone regeneration. *Eur Polym J*. 2019;113:67–77. doi:10.1016/j.eurpolymj.2019.01.042

21. Melnik EV, Shkarina SN, Ivlev SI, et al. In vitro degradation behaviour of hybrid electrospun scaffolds of polycaprolactone and strontium-containing hydroxyapatite microparticles. *Polym Degrad Stab*. 2019;167:21–32. doi:10.1016/j.polymdegradstab.2019.06.017

22. Shkarina S, Shkarin R, Weinhardt V, et al. 3D biodegradable scaffolds of polycaprolactone with silicate-containing hydroxyapatite microparticles for bone tissue engineering: high-resolution tomography and in vitro study. *Sci Rep*. 2018;8:8907. doi:10.1038/s41598-018-27097-7

23. Gorodzha SN, Muslimov AR, Syromotina DS, et al. A comparison study between electrospun polycaprolactone and piezoelectric poly (3-hydroxybutyrate-co-3-hydroxyvalerate) scaffolds for bone tissue engineering. *Colloids Surf B Biointerfaces*. 2017;160:48–59. doi:10.1016/j.colsurfb.2017.09.004

24. Marino A, Tonda-Turo C, Pasquale DD, et al. Gelatin/nanoceria nanocomposite fibers as antioxidant scaffolds for neuronal regeneration. *Biochim Biophys Acta Gen Subj*. 2017;1861:386–395. doi:10.1016/j.bbagen.2016.11.022

25. Jain A, Behera M, Mahapatra C, Sundaresan NR, Chatterjee K. Nanostructured polymer scaffold decorated with cerium oxide nanoparticles toward engineering an antioxidant and anti-hypertrophic cardiac patch. *Mater Sci Eng C*. 2021;118:111416. doi:10.1016/j.msec.2020.111416

26. Asghar MS, Li J, Ahmed I, et al. Antioxidant, and enhanced flexible nano porous scaffolds for bone tissue engineering applications. *Nano Select*. 2021;2:1356–1367. doi:10.1002/nano.202000261

27. Yang MY, Guo ZZ, Li T, et al. Synergetic effect of chemical and topological signals of gingival regeneration scaffold on the behavior of human gingival fibroblasts. *J Biomed Mater Res A*. 2019;107(9):1875–1885. doi:10.1002/jbm.a.36708

28. Negrini NC, Volponi AA, Higgins CA, Sharpe PT, Celiz AD. Scaffold-based developmental tissue engineering strategies for ectodermal organ regeneration. *Mater Today Bio*. 2021;10:100107. doi:10.1016/j.mtbio.2021.100107

29. Gong TX, Li TY, Meng LS, et al. Fabrication of piezoelectric Ca-P-Si-doped PVDF scaffold by phase-separation-hydration: material characterization, in vitro biocompatibility and osteoblast redifferentiation. *Ceram Int*. 2022;48(5):6461–6469. doi:10.1016/j.ceramint.2021.11.190

30. Sola A, Bertacchini J, D'Avella D, et al. Development of solvent-casting particulate leaching (SCPL) polymer scaffolds as improved three-dimensional supports to mimic the bone marrow niche. *Mater Sci Eng C Mater Biol Appl*. 2019;96:153–165. doi:10.1016/j.msec.2018.10.086

31. Hirota M, Shima T, Sato I, et al. Development of a biointegrated mandibular reconstruction device consisting of bone compatible titanium fiber mesh scaffold. *Biomaterials*. 2016;75:223–236. doi:10.1016/j.biomaterials.2015.09.034

32. Jiang J, Li ZR, Wang HJ, et al. Expanded 3D nanofiber scaffolds: cell penetration, neovascularization, and host response. *Adv Healthcare Mater*. 2016;5(23):2993–3003. doi:10.1002/adhm.201600808

33. Chen YJ, Jia ZH, Shafiq M, et al. Gas foaming of electrospun poly (L-lactide-co-caprolactone)/silk fibroin nanofiber scaffolds to promote cellular infiltration and tissue regeneration. *Colloids Surf B Biointerfaces*. 2021;201:111637. doi:10.1016/j.colsurfb.2021.111637

34. Kaplan B, Merdler U, Szklanny AA, et al. Rapid prototyping fabrication of soft and oriented polyester scaffolds for axonal guidance. *Biomaterials*. 2020;251:120062. doi:10.1016/j.biomaterials.2020.120062

35. Taghizadeh M, Taghizadeh A, Yazdi MK, et al. Chitosan-based inks for 3D printing and bioprinting. *Green Chem*. 2022;24(1):62–101. doi:10.1039/D1GC01799C

36. Agarwal T, Hann SY, Chiesa I, et al. 4D printing in biomedical applications: emerging trends and technologies. *J Mater Chem B*. 2021;9(37):7608–7632. doi:10.1039/D1TB01335A

37. Akbarzadeh R, Yousefi AM. Effects of processing parameters in thermally induced phase separation technique on porous architecture of scaffolds for bone tissue engineering. *J Biomed Mater Res B Appl Biomater*. 2014;102(6):1304–1315. doi:10.1002/jbm.b.33101

38. Xu Y, Zhang D, Wang ZL, Gao ZT, Zhang PB, Chen XS. Preparation of porous nanocomposite scaffolds with honeycomb monolith structure by one phase solution freeze-drying method. *Chin J Poly Sci*. 2011;29(2):215–224. doi:10.1007/s10118-010-1015-5

39. Hong ZK, Zhang PB, Liu AX, Chen L, Chen XS, Jing XB. Composites of poly (lactide-co-glycolide) and the surface modified carbonated hydroxyapatite nanoparticles. *J Biomed Mater Res A*. 2007;81(3):515–522. doi:10.1002/jbm.a.31038

40. Kothapalli CR, Shaw MT, Wei M. Biodegradable HA-PLA 3-D porous scaffolds: effect of nano-sized filler content on scaffold properties. *Acta Biomater*. 2005;1(6):653–662. doi:10.1016/j.actbio.2005.06.005

41. Cui Y, Liu Y, Cui Y, Jing XB, Zhang PBA, Chen XS. The nanocomposite scaffold of poly (lactide-co-glycolide) and hydroxyapatite surface-grafted with L-lactic acid oligomer for bone repair. *Acta Biomater*. 2009;5(7):2680–2692. doi:10.1016/j.actbio.2009.03.024

42. Wang ZL, Chen L, Wang Y, Chen XS, Zhang PB. Improved cell adhesion and osteogenesis of op-HA/PLGA composite by poly (dopamine)-assisted immobilization of collagen mimetic peptide and osteogenic growth peptide. *ACS Appl Mater Interfaces*. 2016;8(40):26559–26569. doi:10.1021/acsami.6b08733

43. Hammes MV, Englert AH, Norena CPZ, Cardozo NSM. Effect of water activity and gaseous phase relative humidity on microcrystalline cellulose water contact angle measured by the Washburn technique. *Colloids Surf a Physicochem Eng Asp*. 2016;500:118–126.

44. Xu XL, Chen XS, Ma PA, Wang XR, Jing XB. The release behavior of doxorubicin hydrochloride from medicated fibers prepared by emulsion-electrospinning. *Eur J Pharm Biopharm*. 2008;70(1):165–170. doi:10.1016/j.ejpb.2008.03.010

45. Hanna H, Mir LM, Andre FM. In vitro osteoblastic differentiation of mesenchymal stem cells generates cell layers with distinct properties. *Stem Cell Res Ther*. 2018;9:203. doi:10.1186/s13287-018-0942-x

46. Zhang PB, Hong ZK, Yu T, Chen XS, Jing XB. In vivo mineralization and osteogenesis of nanocomposite scaffold of poly (lactide-co-glycolide) and hydroxyapatite surface-grafted with poly (L-lactide). *Biomaterials*. 2009;30(1):58–70. doi:10.1016/j.biomaterials.2008.08.041

47. Zhang ZZ, Wang SJ, Zhang JY, et al. 3D-printed poly (epsilon-caprolactone) scaffold augmented with mesenchymal stem cells for total meniscal substitution: a 12- and 24-week animal study in a rabbit model. *Am J Sports Med*. 2017;45(7):1497–1511. doi:10.1177/0363546517691513

48. Lane JM, Sandhu HS. Current Approaches to Experimental Bone-Grafting. *Orthop Clin North Am*. 1987;18(2):213–225. doi:10.1016/S0030-5898(20)30385-0

49. Tan BS, Gan SL, Wang XM, Liu WY, Li XM. Applications of 3D bioprinting in tissue engineering: advantages, deficiencies, improvements, and future perspectives. *J Mater Chem B*. 2021;9(27):5385–5413. doi:10.1039/D1TB00172H

50. Eftekhari A, Dizaj SM, Sharifi S, et al. The use of nanomaterials in tissue engineering for cartilage regeneration; current approaches and future perspectives. *Int J Mol Sci*. 2020;21:536. doi:10.3390/ijms21020536

51. Zhang YG, Zhang MM, Cheng DR, et al. Applications of electrospun scaffolds with enlarged pores in tissue engineering. *Biomater Sci*. 2022;10 (6):1423–1447. doi:10.1039/D1BM01651B

52. Ahmadian E, Dizaj SM, Eftekhari A, et al. The potential applications of hyaluronic acid hydrogels in biomedicine. *Drug Res*. 2020;70:6–11. doi:10.1055/a-0991-7585

53. Mohanty S, Larsen LB, Trifol J, et al. Fabrication of scalable and structured tissue engineering scaffolds using water dissolvable sacrificial 3D printed moulds. *Mater Sci Eng C Mater Biol Appl*. 2015;55:569–578. doi:10.1016/j.msec.2015.06.002

54. Samiei M, Aghazadeh M, Alizadeh E, et al. Osteogenic/odontogenic bioengineering with co-administration of simvastatin and hydroxyapatite on poly caprolactone based nanofibrous scaffold. *Adv Pharm Bull*. 2016;6(3):353–365. doi:10.15171/apb.2016.047

55. Rahmati M, Silva EA, Reseland JE, Heyward CA, Haugen HJ. Biological responses to physicochemical properties of biomaterial surface. *Chem Soc Rev*. 2020;49(15):5178–5224. doi:10.1039/d0cs00103a

56. Zhang Y, Wang P, Jin JY, et al. In silico and in vivo studies of the effect of surface curvature on the osteoconduction of porous scaffolds. *Biotechnol Bioeng*. 2022;119(2):591–604. doi:10.1002/bit.27976

57. Fan B, Guo Z, Li XK, et al. Electroactive barium titanate coated titanium scaffold improves osteogenesis and osseointegration with low-intensity pulsed ultrasound for large segmental bone defects. *Bioact Mater*. 2020;5(4):1087–1101. doi:10.1016/j.bioactmat.2020.07.001

58. Satyam A, Tsokos MG, Tresback JS, Zeugolis DI, Tsokos GC. Cell-derived extracellular matrix-rich biomimetic substrate supports podocyte proliferation, differentiation, and maintenance of native phenotype. *Adv Funct Mater*. 2020;30(44):1908752. doi:10.1002/adfm.201908752

59. Wang LY, Yang QH, Huo MF, et al. Engineering single-atomic iron-catalyst-integrated 3D-printed bioscaffolds for osteosarcoma destruction with antibacterial and bone defect regeneration bioactivity. *Adv Mater*. 2021;33(31):2100150. doi:10.1002/adma.202100150

60. Kim YH, Kim DH, Lim H, Baek DY, Shin HK, Kim JK. The anti-inflammatory effects of methylsulfonylmethane on lipopolysaccharide-induced inflammatory responses in murine macrophages. *Biol Pharm Bull*. 2009;32(4):651–656. doi:10.1248/bpb.32.651

61. Takeuchi A, Yamamoto S, Narai R, et al. Determination of dimethyl sulfoxide and dimethyl sulfone in urine by gas chromatography-mass spectrometry after preparation using 2,2-dimethoxypropane. *Biomed Chromatogr*. 2010;24(5):465–471. doi:10.1002/bmc.1313

62. Zou L, Hu L, Pan PP, et al. Icariin-releasing 3D printed scaffold for bone regeneration. *Compos B Eng*. 2022;232:109625. doi:10.1016/j.compositesb.2022.109625

63. Wang SY, Gu RL, Wang FL, et al. 3D-printed PCL/Zn scaffolds for bone regeneration with a dose-dependent effect on osteogenesis and osteoclastogenesis. *Mater Today Bio*. 2022;13:100202. doi:10.1016/j.mtbio.2021.100202

64. Ghandforoushan P, Hanaee J, Aghazadeh Z, et al. Enhancing the function of PLGA-collagen scaffold by incorporating TGF-β1-loaded PLGA-PEG-PLGA nanoparticles for cartilage tissue engineering using human dental pulp stem cells. *Drug Deliv Transl Res*. 2022. doi:10.1007/s13346-13022-01161-13342

65. Wang ZL, Xu Y, Wang Y, Ito Y, Zhang PB, Chen XS. Enhanced in vitro mineralization and in vivo osteogenesis of composite scaffolds through controlled surface grafting of L-lactic acid oligomer on nanohydroxyapatite. *Biomacromolecules*. 2016;17(3):818–829. doi:10.1021/acs.biomac.5b01543